

# JOURNAL OF SUSTAINABLE ENGINEERING AND TECHNOLOGY

JOURNAL OF SUSTAINABLE ENGINEERING AND TECHNOLOGY POSTT

Journal homepage: www.joset.com.ng

# The significance of a window function in the modeling of HP TiO<sub>2</sub> memristor: Pros and Cons

Aliyu Isah<sup>1,2</sup>, Faiza Ali Umar<sup>1</sup> and Jean-Marie Bilbault<sup>2</sup>
<sup>1</sup>Department of Electrical Engineering, Faculty of Engineering, Kano University of Science and Technology,
P.M.B. 3244, Wudil, Kano, Nigeria

<sup>2</sup>ImViA, Université de Bourgogne, BP 21078, Dijon CEDEX, France

# **ARTICLE INFO**

Article History

Received: 28 Nov 2024 Accepted: 03 Mar 2025 Published: 18 April 2025

## **Corresponding Author:**

Aliyu Isah KUST, Wudil aliyuisahbabanta@gmail.com

# **ABSTRACT**

Memristor chips are too expensive and not readily available. Hence, memristor modelling is one of the most important research areas on memristor because it helps to emulate its actual characteristics enabling testing, evaluation and validation of memristor-based applications. The most predominantly used model is the TiO<sub>2</sub> memristor model owing to its simpler modelling equations and easy to fabricate for in-house experiments and characterizations. There are two types of TiO<sub>2</sub> memristor model, viz: linear dopant drift model and nonlinear dopant drift model. The linear dopant drift model suffers hard switching and this issue is avoided in nonlinear model with the aid of a window function. Here it is demonstrated that the window function is added to fix the computational limitation of linear model but it lacks physical meaning. It is further emphasized that modifying the linear model is the most realistic approach to model the actual characteristics of TiO<sub>2</sub> memristor.

**Keywords**: TiO<sub>2</sub> Memristor · Modelling · Window function · Constitutive Relation · Responses

# 1. Introduction

Memory resistor with the moniker "Memristor" is simply a resistor with memory whose electrical property depends on the history of charge having flowed through it. Memristor was initially mistaken as the fourth fundamental passive circuit element, complementing the three existing fundamental circuit elements, namely resistor R, capacitor C and inductor L [1]. However, it was letter proved that memristor cannot be the fourth fundamental passive circuit element but rather a locally active circuit element that reflect the memory effect of resistor [2] [3]. Recall that there are four circuit variables in electrical and electronic engineering, namely: voltage v, current i, magnetic flux  $\phi$  and electric charge q. These circuit variables are related by the time derivatives or in the integral forms as follows.

$$v = \frac{d\phi}{dt} \quad or \quad \phi = \int_{-\infty}^{t} v(\tau) \, d\tau, \tag{1}$$

and

Isah et al.

$$i = \frac{dq}{dt} \quad or \quad q = \int_{-\infty}^{t} i(\tau) \, d\tau. \tag{2}$$

The pair of these circuit variables gives the constitutive relationships defining the phenomenological constants R, C and L which are undoubtedly the three familiar basic passive circuit elements. That is,  $v=R\cdot i$ ,  $\phi=L\cdot i$  and  $q=C\cdot v$  for resistor, capacitor and inductor respectively. The argumentation for the existence of the missing circuit element arose from the tetrahedral symmetry in Figure 1, in which it is claimed there is missing circuit element with the constitutive relation  $f(\phi,q)=0$  i.e  $\phi=M\cdot q$ , where M is a phenomenological constant called memristor with memristance (memory resistance) as its electrical property. The memristance refers to the characteristic of a memristor in which its resistance increases if current (or charge) flow through it in one direction and decreases if the current (or charge) flows in the opposite direction.

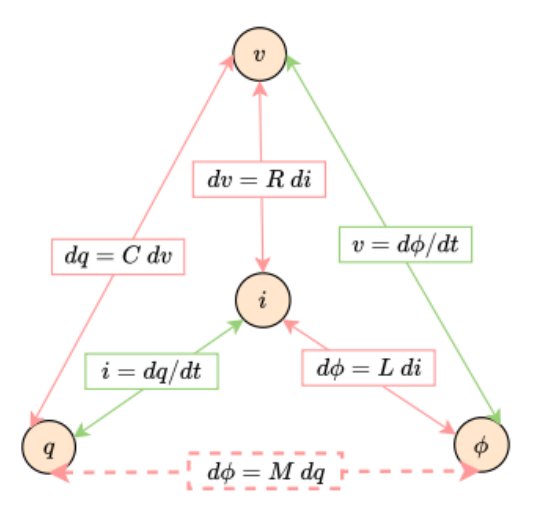


Figure 1. Symmetry arguments for the existence of memristor.

Since the proclamation of the memristor existence in 1971 by Leon Chua [1], it was only realized in 2008 by scientists from HP laboratory [4]. Hence, the HP memristor is known as the  $TiO_2$  memristor because it uses  $TiO_2$  material sandwiched between two platinum electrodes, see Figure 2. The most prominent signature of a memristor is its pinched hysteresis loop (PHL) in the v-i plane whose lobe area decreases with increase in input frequency. One of the critiques of the existence of memristor is the manifestations of PHL in natural phenomena such as plant and other nonlinear dynamical system, however, a simple test was proposed to identify memristor from other nonlinear dynamical systems [5] [6]. Despite the published findings about solid state memristor and many proposed applications by HP lab, there are no memristor chips to buy from HP. Fortunately, one can purchase self-directed channel (SDC) memristor chip from KNOWM.org but it is too expensive [7] [8]. This is the reason why memristor modeling is one of the key research areas about memristive systems. The memristor modeling techniques help to develop model with approximate characteristic of a memristor enabling testing and validation of memristor-based applications.

TiO<sub>2</sub> memristor has two models, namely, linear dopant drift and nonlinear dopant drift models. The linear model suffers boundary problems, hence the different between the two is the introduction of a window function allowing to fix the boundary issues. Here, it is however emphasized that the boundary issue is the limitation of the linear model and instead of adding a window function, the linear model can be modified. The addition of a window function fixes the boundary issue, but it also enforces different memristance dynamic which may likely cause dilemma in choosing the most suitable model. Hence, the window function is added to fix the mathematical limitation of the linear model. Here, a new model is proposed and it does not require a window function. This paper presents the modeling technique of HP TiO<sub>2</sub> memristor and the impact of window function. The models are compared with the proposed model of memristor, and the fingerprints of a memristor are observed.

#### 2. Modelling of TiO<sub>2</sub> memristor

There are many fingerprints of a memristor, and these are the signatures use to identify memristive device from other nonlinear dynamical systems that may be confused as memristive systems [9] [10] [11] [12]. However, there are three eminent fingerprints of memristor. Firstly, the i-v response of a memristor is a Lissajous figure in the first and third quadrants of v-i plane and it is pinched at the origin, meaning, v = 0 if i = 0 and vice versa. Secondly, the lobe area of the pinched hysteresis loop decreases with increase in input frequency. Thirdly, when the input frequency is infinite, the lobe area disappears, hence the PHL reduces to a linear graph resembling the characteristic of ordinary linear resistor. Therefore, at infinite input frequency, memristor is not different from ordinary resistor because the lobe area is the manifestation of its memory effect, hence just leaving behind the resistive effect.

Memristor modeling entails imitating the actual characteristic of a memristor, mainly focuses on its main signatures. Figure 2 shows the formation of  $TiO_2$  and its modeling illustration. The deposition process consists of  $TiO_2$  material of width D sandwiched between two platinum electrodes. One side of the  $TiO_2$  is doped with some positive oxygen vacancies allowing to create more charges carriers, hence improving the conductivity of the doped region. The deposited material undergoes electroforming process thereby creating an imaginary boundary between the doped region of width w and the undoped region having width D-w, each having a resistance  $R_{on}^*$  and  $R_{off}^*$  respectively. Depending on the magnitude and polarity of the applied voltage or current signal, the imaginary boundary moves back and forth corresponding to the increase and decrease of w which result in varying the effective resistance of the device. Therefore, w is the state variable of the device, hence the arrangement resembles two variable resistors with their resistances determine by w. Looking at the dimension of  $TiO_2$  and the corresponding variation of w, it can be seen that  $R_{on}^* = \frac{w}{D}R_{on}$  and  $R_{off}^* = \frac{D-w}{D}R_{off}$ , where  $R_{on}$  and  $R_{off}$  are the two limiting resistance states, i.e. the lowest and highest resistance that the device can reach. In other words,  $R_{on}$  and  $R_{off}$  refer to the conductive region (ON state) and less conductive region (OFF state), which corresponds to the case when the device is wholly doped and partially doped respectively.

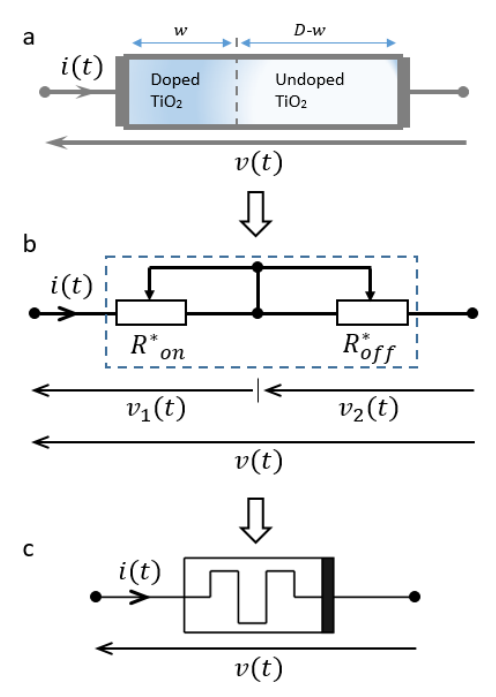


Figure 2. Schematic illustration of TiO<sub>2</sub> memristor. (a) Fabrication, (b) Modeling and (c) Symbol.

Now, v(t) is the voltage across the electrodes, let the implicit voltage drops across  $R_{on}^*$  and  $R_{off}^*$  be  $v_1(t)$  and  $v_2(t)$  respectively, such that:

$$v_1(t) = R_{on}^* \cdot i(t) = \frac{w}{D} R_{on} \cdot i(t) = \frac{w R_{on}}{w R_{on} + (D - w) R_{off}} v(t), \tag{3}$$

and

$$v_2(t) = R_{off}^* \cdot i(t) = \frac{D - w}{D} R_{off} \cdot i(t) = \frac{(D - w) R_{off}}{w R_{on} + (D - w) R_{off}} v(t). \tag{4}$$

From equation (3) and (4), it can be seen that  $v(t) = v_1(t) + v_2(t)$ , this gives the port equation as follows:

$$v(t) = \left(\frac{w}{D}R_{on} + \frac{D - w}{D}R_{off}\right) \cdot i(t) = M(w) \cdot i(t),\tag{5}$$

where:

$$M(w) = \frac{w}{D}R_{on} + \frac{D - w}{D}R_{off}.$$
 (6)

M(w) is the memristance in Ohms  $(\Omega)$ . If u is the speed of the boundary which corresponds to the speed of the dopants as they drift due to the applied current or voltage signal, then  $u = \mu_v E$ , where  $\mu_v$  is the dopant mobility and E is the electric field in the conductive region. The dopants have to move through a distance given by the width (w) of the conductive region, hence  $u=\frac{dw}{dt}=\mu_{v}E$ . It implies that:  $E=\frac{1}{\mu_{v}}\frac{dw}{dt}.$ 

$$E = \frac{1}{\mu_v} \frac{dw}{dt}.\tag{7}$$

Considering the relation between the electric field and electric potential, it can be seen that  $E = \frac{dv_1}{dv_1}$ . The electric

field 
$$E$$
 in the conductive region can be expressed using equation (3) as:
$$E = \frac{v_1(t)}{w} = \frac{R_{on} \ v(t)}{w \ R_{on} + (D - w) \ R_{off}} = \frac{R_{on}}{D} \ i(t). \tag{8}$$

$$\frac{dw}{dt} = \frac{\mu_v R_{on}}{D} i(t). \tag{9}$$

Equations (5) and (9) give the model of the TiO<sub>2</sub> memristor and can be rearranged to give the following set of equations:

$$\begin{cases} v(t) = M(w) \ i(t), \\ \frac{dw}{dt} = \frac{\mu_v R_{on}}{D} \ i(t). \end{cases}$$
 (10)

The model (10) can be simplified further by introducing normalized state variable as  $x = \frac{w}{D}$ . Recall that wincreases and decreases depending on the moving direction of the boundary. Hence, if  $w = 0 \Rightarrow x = 0$  and if  $w = D \Rightarrow x = 1$ . Therefore, the normalized state variable is in the interval [0, 1], hence equation (10) can be rewritten in normalized form as:

$$\begin{cases} v(t) = M(x) \ i(t), \\ \frac{dx}{dt} = \frac{\mu_{v} R_{on}}{D^{2}} \ i(t), & x \in [0, 1] \\ M(x) = R_{off} - \delta R \ x. & M \in [R_{off}, R_{on}] \end{cases}$$
(11)

Integrating the state equation in (11) and setting the initial conditions of x and q as zero, it becomes:

$$x = \frac{\mu_v R_{on}}{D^2} q(t), \tag{12}$$

which is a simple linear relationship between the state variable x and the flowing charge q(t), hence it is called the linear dopant drift model. The speed of the boundary between the doped and the undoped regions decreases as it approaches either of the edge boundaries i.e. x = 0 or x = 1. This causes discontinuity at the boundaries. The bulk of the memristor dynamic is observed for x being in the interval 0 < x < 1. Therefore, the linear dopant drift model has boundary issue because it does not take into account the cases x = 0 and x = 1 as would be explored further in the following section.

The evolution of the state variable x corresponds to the coordinate of the boundary between the doped and the undoped regions and it is determined by the flowing charge, as confirmed by equation (12). Recall that x = 1 refers to the condition in which the device is fully doped, hence the memristance becomes  $R_{on}$ . Therefore, the amount of charge required to achieved this condition is called a charge scaling factor Qand it is determined by substituting x=1 in equation (12). Thus:  $x=1=\frac{\mu_{\nu}R_{on}}{D^2}Q\Rightarrow Q=\frac{D^2}{\mu_{\nu}R_{on}}$ . Therefore, substituting Q into (12), the relationship between the state variable x and the flowing charge q becomes:

$$x(t) = \frac{q(t)}{0}. (13)$$

Since x is bounded in the interval [0, 1], therefore from equation (13), for q(t) = 0,  $x(t) = 0 \Rightarrow M(x) = M(q) = 0$  $R_{off}$ . Likewise, for q(t) = Q,  $x(t) = 1 \Rightarrow M(x) = M(q) = R_{on}$ . Hence, the linear model (12) can be rewritten in terms of q(t), thus:

Isah et al.

$$\begin{cases} v(t) = M(q) \cdot i(t), \\ \frac{dx}{dt} = \frac{1}{Q} i(t), & for \ 0 < x < 1 \\ M(q) = R_{off} - \delta R \frac{q}{Q}. & for \ 0 < q < Q \end{cases}$$
(14)

From the state equation (14), the state variable is simplified to give:

$$x - x_0 = \frac{1}{O}(q - q_0),$$

where  $x_0$  is the initial coordinate of the state variable and  $q_0$  is the last amount of charge having flowed previously through the memristor. In fact,  $q_0$  reflects the memory effect of memristor and it is what determined the initial memristance. With x known, M(x) can be determined and all other variables could be determined accordingly. Therefore, using a sinusoidal input current source with amplitude 0.25mA, Figure 3 shows the response of the linear model given by equation (14) and it is the typical current-voltage characteristic of a memristor. The i-v characteristic of a memristor is always a pinched hysteresis loop as shown in Fig. 3b and it is the most prominent fingerprint of a memristor [11] [12].

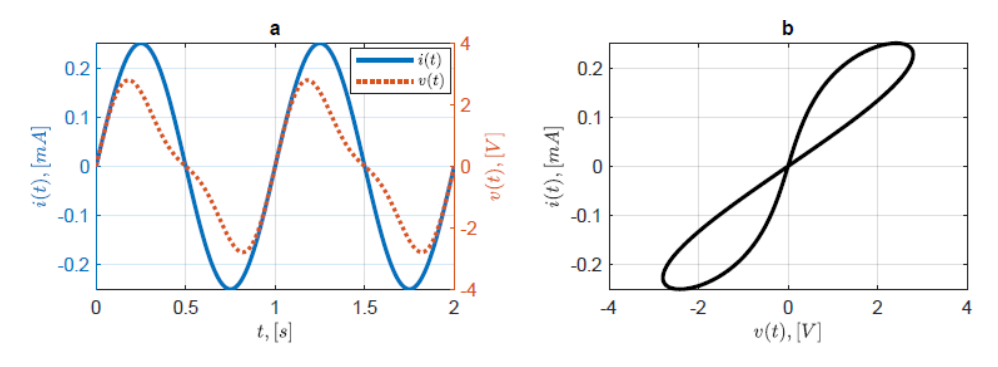


Figure 3: The response of the linear model, equation (14), showing the typical current-voltage characteristic of a memristor.

Notice that the state equation in (14) shows that the state variable x is just a function of the flowing charge q, thus characterizing an ideal charge-controlled memristor. It can be seen that  $M(q) = R_{off}$  if  $q \le 0$  and  $M(q) = R_{on}$  if  $q \ge Q$ . Moreover, from equation (14), the memristance transition with respect to the flowing charge can be expressed as:

$$\frac{dM(q)}{dq} = -\frac{\delta R}{Q}.$$
 (fixed)

This gives the slope of the result in Figure 4 and it is a linear characteristic having a slope  $-\frac{\delta R}{Q}$ . At the boundary q=0 and q=Q, it is expected to have zero dopants drift so that the memristance can assume values  $R_{off}$  and  $R_{on}$  respectively. Unfortunately, this feature is missing in the Linear dopant drift model, hence there is discontinuity in the memristance transition at q=0 and q=Q as shown in Figure~4. In fact, while simulating the linear model in SPICE (Simulation Program for Integrated Circuit Emphasis), there is always a computational error when the amplitude of the applied current or voltage signal is substantially enough to force the state variable x to reach the boundary 0 or 1. Therefore, it becomes necessary to modify the boundary condition of the linear model and this is done by adding a window function f(x), as presented in section 3. The window function enforces a zero dopants drift at the boundary. The result in Figure~4 is obtained for values of parameters according to [4], that is  $R_{off}=16K\Omega$ ,  $R_{on}=100\Omega$ , D=10nm,  $\mu_v=10^{-10}cm^2/V$ . s, which gives  $Q=\frac{D^2}{\mu_v R_{on}}=100\mu C$ .

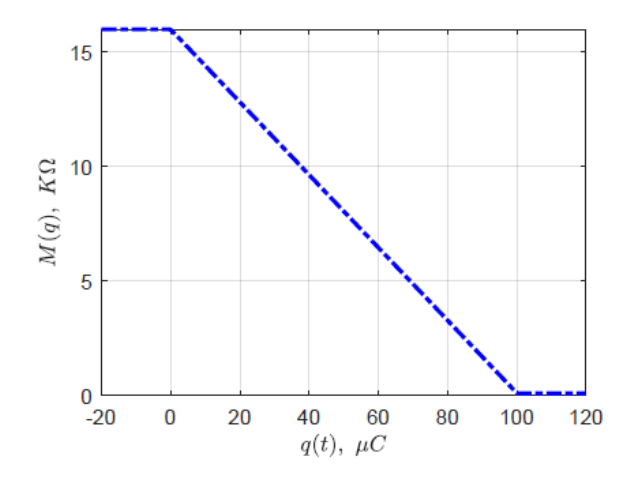


Figure 4: Memristance transition of the linear dopant model. There is discontinuity at q = 0 and q = Q.

# 3. Nonlinear dopant drift modelling

As described by equation (12), the state variable x is proportional to the flowing charge q through the memristor and it also corresponds to the dynamic of the dopants as they drift upon the application of voltage or current signal. From the relation  $u = \frac{dw}{dt'}$  it can be observed that the drift speed of the dopants decreases to zero as they approach either of the boundary i.e. x = 0 or x = 1 and this exactly the point where the memristance transition changes state from  $R_{off}$  (OFF state) to  $R_{on}$  (ON state) and vice-versa. Hence, it requires a high voltage or current to achieve the memristance transition at the boundary and this condition is called a **hard switching**. Thus, the hard switching causes discontinuity (see Figure 4) at the boundaries and this is undesirable. To avoid this scenario, different boundary conditions are applied allowing to specify the hard switching. To apply the boundary conditions, a window function f(x) is applied to the righthand side of the state equation (11) and the model becomes:

$$\begin{cases} v(t) = M(x) \ i(t), \\ \frac{dx}{dt} = \frac{\mu_{v} R_{on}}{D^{2}} f(x) \ i(t), & x \in [0, 1] \\ M(x) = R_{off} - \delta R \ x. & M \in [R_{off}, R_{on}] \end{cases}$$
(15)

Note that f(x) must be a dimensionless quantity added to impose zero dopants drift at the boundary where x = 0 and x = 1, hence it causes a nonlinear dopant drift at these boundaries. Therefore, equation (15) is called the **nonlinear dopant drift model** and is more accurate than the linear dopant drift model. The nonlinear dopant drift model (15) is used to create memristor component in SPICE circuit simulators because it gives no computational errors [13]. There are many proposed f(x) for nonlinear dopant drift modeling and here are the prominent ones. Strukov et al. proposed f(x) as [4]:

$$f(x) = x(1-x). (16)$$

Notice that the function f(x = 0) = f(x = 1) = 0, will ensure zero dopants drift at the boundaries until there is change in resistance state of the memristor. This is true for all the proposed f(x). Another commonly used f(x) is the one by Joglekar et al. [14]:

$$f(x) = 1 - (2x - 1)^{2p}, (17)$$

where  $p \in Z^+$  is a control parameter and  $Z^+$  is positive integer. The function f(x) in equation (17) is the improved version of the one in equation (16), because for p=1, then f(x)=4x(1-x), hence the two functions are identical except for the factor 4. Figure 5 compares the memristance transition from  $R_{off}$  to  $R_{on}$  (and vice-versa) for linear dopant drift model and nonlinear dopant drift model using f(x) by Joglekar et al. It clearly shows the effect of varying the control parameter p. Hence as p increases, the dynamic of the nonlinear model approaches that of the linear model.

Isah et al.

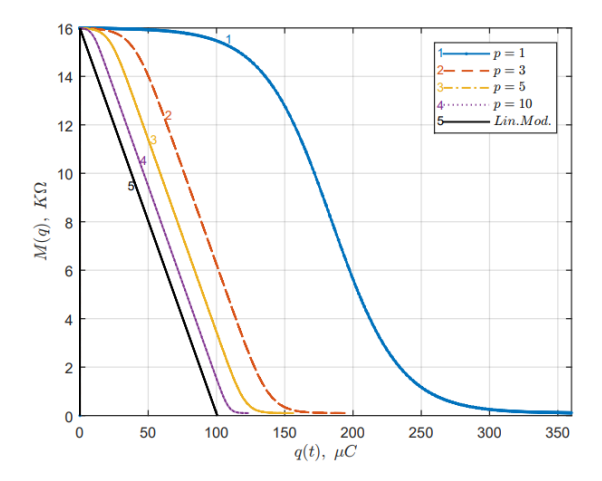


Figure 5. Comparing linear model and nonlinear model (using Joglekar et al. function). The response of the nonlinear dopant drift model approaches linear dopant drift model as  $p \to \infty$ .

Therefore, if p = 1,  $f(x) = 4x(1 - x) \Rightarrow f(x = 0) = f(x = 1) = 0$ . Furthermore, if p = 2,  $f(x) = 1 - (2x - 1)^4 = -16x^4 + 32x^3 + 24x^2 + 8x \Rightarrow f(x = 0) = f(x = 1) = 0$ . From the state equation (15), it can be seen that:

$$\int \frac{dx}{f(x)} = \frac{\mu_{\nu} R_{on}}{D^2} \int i(t) dt.$$

It follows that the larger the control parameter, the more difficult it is to simplify the nonlinear model analytically. For example, using the function proposed by Joglekar et al. with p = 1 i.e. f(x) = 4x(1 - x), and recalling that  $\frac{1}{\rho} = \frac{\mu_{\nu}R_{on}}{D^2}$ , then the state equation (15) is simplified to give:

$$x = \frac{x_0 e^{\frac{4(q-q_0)}{Q}}}{1 - x_0 + x_0 e^{\frac{4(q-q_0)}{Q}}}$$

 $x=\frac{x_0\,e^{\frac{4(q-q_0)}{Q}}}{1-x_0+x_0\,e^{\frac{4(q-q_0)}{Q}}}$  Therefore, if p=2, the equation becomes tedious and it becomes extremely difficult for higher values of p. Similarly, from the equation set (15), with x known, the memristance M(x) can be determined and all the other variables could be determined.

Another commonly used function f(x) is the one proposed by Prodromakis et al. [15], which is stated as follows:

$$f(x) = 1 - [(x - 0.5)^2 + 0.75]^p, (18)$$

or

$$f(x) = j(1 - [(x - 0.5)^2 + 0.75]^p),$$

where j is another control parameter allowing to scale the function up and down. Biolek et al. proposed f(x)as [13]:

$$f(x) = 1 - (x - stp(-i))^{2p}, (19)$$

where:

$$stp(i) = \begin{cases} 1 & for \ i \ge 0 \\ 0 & for \ i < 0 \end{cases}$$

Furthermore, Isah et al. proposed f(x) to be [16]:

$$f(x) = \frac{1}{2} [1 + \cos \pi (2x - 1)]. \tag{20}$$

All of these functions can be used to specify the boundary conditions. Figure 6 compares the response of nonlinear model using window functions by Strukov et al., Joglekar et al. and Prodromakis et al. Notably, Biolek et al. developed SPICE netlist file of memristor for creating memristor component in SPICE [13]. In fact, recent SPICE circuit simulators have already incorporated memristor component. Here, the SPICE netlist file is modified by considering the window functions under consideration. Therefore, three memristor components are created in SPICE by considering the functions proposed by Strukov et al., Joglekar et al. and Prodromakis et al. and the results are shown in Figure 6. The results show that the amount of charge q(t) required to flow for the total field of memristance variation depends on the model under consideration, because each model requires different quantity of charge Q for a full memristance transition. Furthermore, the results show that the dynamic of the memristance transitioning with respect to the flowing charge depends on the window function under consideration.

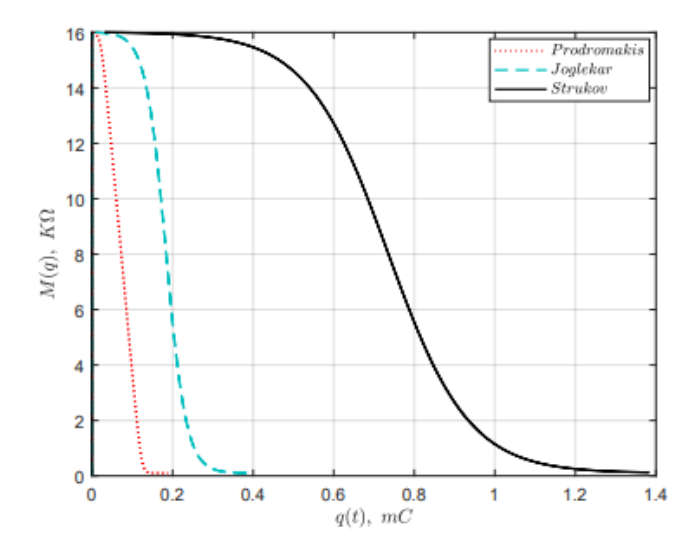


Figure 6. Memristance transition: comparing the response of linear model and the three nonlinear models by Prodromakis et al., Joglekar et al. (for p = 5.) and Strukov et al.

The same values of parameters are used for the results in Figures 4, 5 and 6, however the window functions affect the dynamic of the memristor to the extent that the amount of charge Q required for the full memristance transition depends on the type of function under consideration. Unlike Figure 4, observing Figure 6, it is worth to note that there is no discontinuity on the curve at a point where  $M(q) = R_{off}$  for q = 0 and  $M(q) = R_{on}$  for q = 0 for both the nonlinear models. Figure 7 compares the response of the linear model with nonlinear models using Prodromakis' function. Hence, the evolution of the nonlinear model is continuous at q = 0 and q = 0.

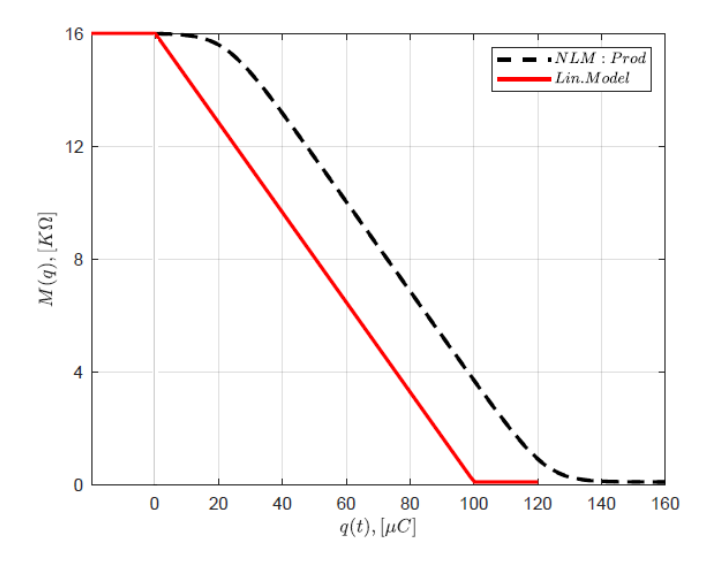


Figure 7: Comparing the response of the linear model (*Lin. Model*) with the nonlinear model using the function by Prodromakis et al. (*NLM: Prod*).

#### 4. Physical effects of window function

As can be observed in Figure 6, it is worth to note that even so the same values of parameters are used for both the nonlinear models, the value of Q for which  $M(q) = R_{on}$  is not the same, hence the memristance dynamic differs as well. The results show that the window function is added to avoid the mathematical limitations of the linear dopant drift model but it has no physical meaning. The mathematical limitations of the linear model are its associated boundary issues, which at times causes computational errors while simulating the model in SPICE. We also remark that the boundary issues of the linear model are manifested by the formed angulations at q=0C and  $q=100\mu C$  of the memristance transition shown in Figures 4 and 7. Although the window function helps to fix the boundary issues of the linear model, however, it has it owns drawbacks. For example, analytically, it is practically impossible to simplify the nonlinear model when the value of the control parameter p is large [14]. Therefore, for a large value of control parameter, the model can only be simplified numerically. By extension, it is too difficult (or rather impossible) to perform analytical interpretation of a large network (such as memristive grids) employing the nonlinear model due to the added window function. Hence, if the linear model can be modified, then it will be a better considerate than resorting to the use of a window function. Therefore, the use of window function can be avoided by improving the linear model to have continuous memristance transition at the boundary for all possible values of q(t). Hence, the modification of the linear model given in equation (14) aims to improve the model so that the discontinuity at q=0 and q=Q(shown in Figures 4 and 7) can be avoided and the response resemble that of the nonlinear model.

The new model is derived from a cubic polynomial by applying the conditions in equation (15) [17]:

$$M(q) = a + b q + c q^2 + d q^3, \quad for q \in [0, Q]$$
 (21)

The coefficients a, b, c and d are constants and are determined as follows. The model takes into account both the dynamic region of operation of the memristor and the boundary problems. The discontinuity in the linear model (21) (and Figure 7) signifies that:

$$\left.\frac{dM(q)}{dq}\right|_{q=0}=\left.\frac{dM(q)}{dq}\right|_{q=0}=0.$$

Therefore, the first derivative of equation (21) with respect to q is:

$$\frac{dM(q)}{dq} = b + 2c q + 3d q^2. {(22)}$$

Notice the outlined conditions in equations (14) and (15), i.e. the limiting resistances  $[R_{off}, R_{on}]$  of the memristance and the corresponding charge evolution [0,Q] for  $R_{off}$  and  $R_{on}$  respectively. Therefore, equations (21) and (22) are simplified simultaneously in order to determine the coefficients a, b, c and d. Hence, for q=0,  $M(q)=R_{off}$  and substituting for q=0 into equation (21), then  $M(q)=a=R_{off}$ . Also substituting q=0 into (22) gives b=0. Likewise, for q=Q,  $M(q)=R_{on}$  and substituting into equation (21), it becomes:

$$M(q) = R_{on} = R_{off} + c Q^2 + d Q^3.$$
 (23)

With a and b known (i.e.  $a=R_{off}$  and b=0), equations (22) and (23) are solved simultaneously to give the other constants:  $c=-\frac{3 \, \delta R}{o^2}$  and  $d=\frac{2 \, \delta R}{o^3}$ . Substituting for these constants into equation (21) gives:

$$M(q) = \begin{cases} R_{off}, & for \ q \le 0 \\ R_{off} - \frac{3 \delta R}{Q^2} q^2 + \frac{2 \delta R}{Q^3} q^3, & for \ 0 \le q \le Q \\ R_{on}. & for \ q \ge Q \end{cases}$$

$$(24)$$

From equation (24), the memristance transition with respect to the flowing charge becomes:

$$\frac{dM(q)}{dq} = -\frac{6\delta R}{Q^2}q + \frac{6\delta R}{Q^3}q^2. \quad (continuous)$$

Hence, by substituting q = 0 and q = Q, it can be seen that:

$$\left.\frac{dM(q)}{dq}\right|_{q=0}=\left.\frac{dM(q)}{dq}\right|_{q=Q}=0.$$

This confirms the zero dopants drift at the boundary and this is exactly the role of the window function. Therefore, the proposed model is the modified linear model manifesting the role of the window function in the nonlinear dopant drift model i.e. equation (15).

Using the values of parameters stated in page 5, so that value of Q will be the same for the linear model and the proposed model, and using a sinusoidal input current source, the response of this model is shown in Figure 8 and it confirms the signature of a memristor. Furthermore, Figure 9 shows the effect of varying the input frequency and the result demonstrate the signatures of a memristor. The comparison of the memristance transition with respect to the flowing charge for the linear dopant drift model (equation (14)) and the modified or proposed linear dopant drift model (equation (24)) is shown in Figure 10. Firstly, Figure 10a shows that the response of the proposed model has no discontinuity and then the comparison of the two models is presented in Figure 10b. Notice that the boundary issues are at q = 0C and  $q = Q = 100\mu C$ . It is also important to note that in the case of the nonlinear model, the value of Q depends strongly on the value of the control parameter P0 as illustrated in Figure 5. This means that the window function also affects the dynamic of the memristance and the model tends to respond differently depending on the window function under consideration, even for the same values of parameters. However, for the same values of parameters, the value of Q1 for the linear model and the proposed model is the same.

The response of the proposed model in Figure 10a shows that the memristance transition at the boundary is similar to the ones in the nonlinear dopant drift model because it has no discontinuity. The new model showcases the typical characteristics of memristor as illustrated in Figures 8 and 9 confirming the model as memristive. Therefore, it has been proven that the very needs of a window function can be achieve without resorting to adding a new function. This has been confirmed from the memristance transition with respect to the flowing charge through the memristor, in which the continuity of the memristance function at q=0 and q=Q of the proposed model is similar to that of the nonlinear model. The proposed model is the most reliable in the dynamic analysis of memristor in neighbourhood connections of a memristive grid network for signal processing [17].

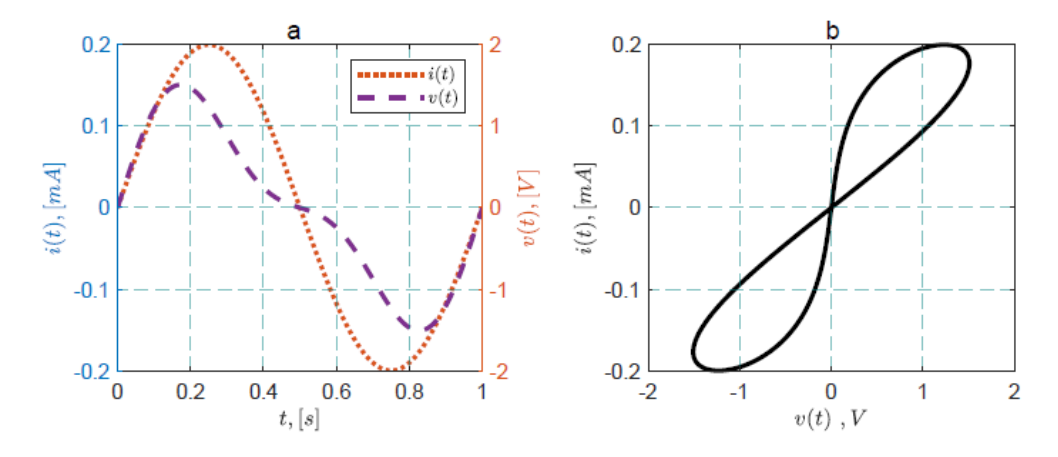


Figure 8: The current-voltage response of the modified linear model.

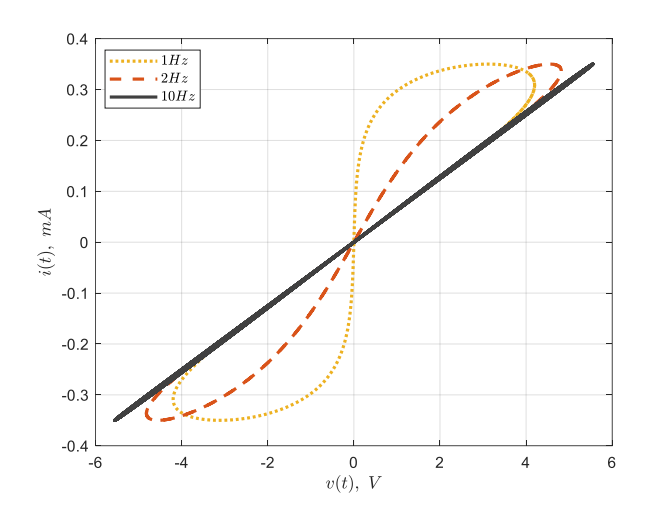


Figure 9: Effect of varying the input frequency.

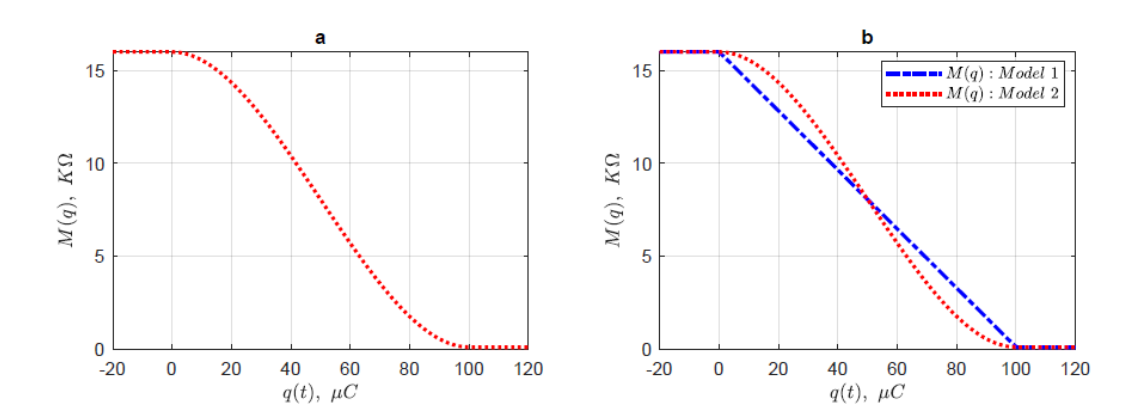


Figure 10: (a) Response of the proposed model: Memristance transition with respect to charge. (b) Comparison of the linear model (Model 1) and the proposed (or modified) model (Model 2).

#### 5. Conclusion

Three models (including the proposed model) of TiO<sub>2</sub> memristor are presented. The linear model is the most realistic approach because it tends to model the physical characteristics of TiO<sub>2</sub> memristor shown in Figure 2. However, the boundary problems became a significant issue in using linear model especially in circuit simulators because there are always computational errors due to boundary problems when the applied voltage is substantially enough to force the state variable to the boundary, that is x = 0 and x = 1. The boundary problems cause hard switching that result in discontinuity of the memristance transition with respect to the flowing charge as manifested by the formed angulation at q = 0 and q = Q. The introduced window function helps to avoid the discontinuity but it lacks physical meaning, because it is normally added to solve the computational limitations associated to the linear dopant drift model. The proposed model is the modified version of the linear dopant drift model and proven to be promising in solving the discontinuity issues without the need of a window function. The pros aspects of a window function include the following. The window function improves the dynamic of the model by varying the transitioning time of the memristor to switch its resistance state from OFF (high resistance state) to ON (low resistance state) and vice-versa. Secondly, it removes the discontinuity at q = 0 and q = Q. The cons aspects of a window function include its non-physical meaning, but only added to solve the mathematical limitation of the linear model. Furthermore, the window functions tend to respond differently. Therefore, one has to choose the best suitable function for the undertaken project or application. In fact, it is tedious or practically impossible to carry out circuit analysis with a function having large value of control parameter p, except with the aid of computer simulation. To avoid any

obscurity related to the choice of a window function, the proposed model is the best option to begin with. The conductance modulation of memristor resembles that of a chemical synapse, hence one of the prominent application areas of memristor is in the electronic modeling of synapse. Optimistically and as pointed out in the reference [17], the proposed model is most suitable in the analytical interpretation of memristor as synapse.

#### 6. References

- [1] L. Chua, "Memristor-the missing circuit element," *IEEE Transactions on circuit theory*, vol. 18, no. 5, pp. 507-519, 1971
- [2] Y.V. Pershin and M. Di Ventra, "Memory effects in complex materials and nanoscale systems," *Advances in Physics*, vol. 60, no. 2, pp. 145-227, 2011.
- [3] M. Di Ventra and Y.V, Pershin, Memristors and Memelements: Mathematics, Physics and Fiction, Springer, 2023.
- [4] D. Strukov, G.S. Snider, D.R. Stewart and R.S. Williams, "The missing memristor found," *nature*, vol. 453, no. 7191, pp. 80-83, 2008.
- [5] Y. Pershin and M. Di Ventra, "A simple test for ideal memristors," *Journal of Physics D: Applied Physics*, vol. 52, no. 1, p. 01LT01, 2018.
- [6] Y. Pershin, J. Kim, T. Datta. and M. Di Ventra, "An experimental demonstration of the memristor test," *Physica E: Low-dimensional Systems and Nanostructures*, vol. 142, p. 115290, 2022.
- [7] K. Campbell, "Self-directed channel memristor for high temperature operation," *Microelectronics journal*, vol. 59, pp. 10-14, 2017.
- [8] K. Campbell, "The self-directed channel memristor: operational dependence on the metal-chalcogenide layer," in *Handbook of Memristor Networks*, 2019, pp. 815-842.
- [9] D. Biolek, Z. Biolek, V. Biolkova and Z. Kolka, "Some fingerprints of ideal memristors," in *IEEE International Symposium on Circuits and Systems (ISCAS)*, 2013.
- [10] S. Adhikari, M.P. Sah, H. Kim, and L.O. Chua, "Three fingerprints of memristor," in *Handbook of Memristor Networks*, 2019, pp. 165-196.
- [11] D. Biolek and Z. Biolek, "About fingerprints of Chua's memristors," *IEEE Circuits and Systems Magazine*, vol. 18, no. 2, pp. 35-47, 2018.
- [12] L. Chua, "Everything you wish to know about memristors but are afraid to ask," in *Handbook of Memristor Networks*, 2019, pp. 89-157..
- [13] Z. Biolek, D. Biolek, and V. Biolkova, "SPICE Model of Memristor with Nonlinear Dopant Drift," *Radioengineering*, vol. 18, no. 2, 2009.
- [14] Y. Joglekar and S.J. Wolf, "The elusive memristor: properties of basic electrical circuits," *European Journal of physics*, vol. 30, no. 4, p. 661, 2009.
- [15] T. Prodromakis, B.P. Peh, C. Papavassiliou and C. Toumazou "A versatile memristor model with nonlinear dopant kinetics," *IEEE transactions on electron devices*, vol. 58, no. 9, pp. 3099-3105, 2011.
- [16] A. Isah and J.M. Bilbault, "Review on the basic circuit elements and memristor interpretation: Analysis, technology and applications," *Journal of Low Power Electronics and Applications*, vol. 12, no. 3, p. 44, 2022.
- [17] A. Isah, A.S.T. Nguetcho, S. Binczak and J.M. Bilbault, "Memristor dynamics involved in cells communication for a 2D non-linear network," *IET Signal Processing*, vol. 14, no. 7, pp. 427-434, 2020.